

**WestminsterResearch**

<http://www.westminster.ac.uk/westminsterresearch>

**Congenital macrothrombocytopenia with focal myelofibrosis due to mutations in human G6b-B is rescued in humanized mice**

**Hofmann, I., Geer, M.J., Vögtle, T., Crispin, A., Campagna, D.R., Barr, A.J., Calicchio, M.L., Heising, S., van Geffen, J.P., Kuijpers, M.J.E., Heemskerk, J.W.M., Eble, J.A., Schmitz-Abe, K., Obeng, E.A., Douglas, M., Freson, K., Pondarré, C., Favier, R., Jarvis, G.E., Markianos, K., Turro, E., Ouwehand, W.H., Mazharian, A., Fleming, M.D. and Senis, Y.**

This is an accepted manuscript of an article originally published in Blood

The final published version is available online at:

<https://dx.doi.org/10.1182/blood-2017-08-802769>

© the American Society of Hematology

---

The WestminsterResearch online digital archive at the University of Westminster aims to make the research output of the University available to a wider audience. Copyright and Moral Rights remain with the authors and/or copyright owners.

---

Whilst further distribution of specific materials from within this archive is forbidden, you may freely distribute the URL of WestminsterResearch: (<http://westminsterresearch.wmin.ac.uk/>).

In case of abuse or copyright appearing without permission e-mail [repository@westminster.ac.uk](mailto:repository@westminster.ac.uk)

## **Congenital macrothrombocytopenia with focal myelofibrosis due to mutations in human G6b-B is rescued in humanized mice**

Inga Hofmann,<sup>1,2\*</sup> Mitchell J. Geer,<sup>3\*</sup> Timo Vögtle,<sup>3</sup> Andrew Crispin,<sup>2</sup> Dean R. Campagna,<sup>2</sup> Alastair Barr,<sup>4</sup> Monica L. Calicchio,<sup>2</sup> Silke Heising,<sup>3</sup> Johanna P. van Geffen,<sup>5</sup> Marijke J. E. Kuijpers,<sup>5</sup> Johan W. M. Heemskerk,<sup>5</sup> Johannes A. Eble,<sup>6</sup> Klaus Schmitz-Abe,<sup>7</sup> Esther A. Obeng,<sup>8</sup> Michael Douglas,<sup>9-11</sup> Kathleen Freson,<sup>12</sup> Corinne Pondarré,<sup>13</sup> Rémi Favier,<sup>14,15</sup> Gavin E. Jarvis,<sup>16</sup> Kyriacos Markianos,<sup>2</sup> Ernest Turro,<sup>17</sup> Willem H. Ouwehand,<sup>18-20</sup> Alexandra Mazharian,<sup>3</sup> Mark D. Fleming,<sup>2\*</sup> and Yotis A. Senis<sup>3\*</sup>

<sup>1</sup>Division of Hematology, Oncology, Bone Marrow Transplantation, Department of Pediatrics, University of Wisconsin, Madison, WI, USA

<sup>2</sup>Department of Pathology, Boston Children's Hospital, Boston, MA, USA

<sup>3</sup>Institute of Cardiovascular Sciences, College of Medical and Dental Sciences, University of Birmingham, Birmingham, UK

<sup>4</sup>Department of Biomedical Science, University of Westminster, London, UK

<sup>5</sup>Department of Biochemistry, Cardiovascular Research Institute Maastricht, Maastricht University, Maastricht, The Netherlands

<sup>6</sup>Institute of Physiological Chemistry and Pathobiochemistry, University of Münster, Münster, Germany

<sup>7</sup>Division of Genetics and Genomics, Boston Children's Hospital, Boston, MA, USA

<sup>8</sup>Dana-Farber/Boston Children's Cancer and Blood Disorders Center, Harvard Medical School, Boston, MA, USA

<sup>9</sup>Institute of Inflammation and Ageing, College of Medical and Dental Sciences, University of Birmingham, Birmingham, UK

<sup>10</sup>Department of Neurology, Dudley Group NHS Foundation Trust, Russells Hall Hospital, Dudley, UK

<sup>11</sup>School of Life and Health Sciences, Aston University, Birmingham, UK

<sup>12</sup>Department of Cardiovascular Sciences, University of Leuven, Leuven, Belgium

<sup>13</sup>Department of Pediatrics, and INSERM Unité 955, Paris-Est Créteil University, Créteil, France

<sup>14</sup>Assistance Publique-Hôpitaux de Paris, French reference centre for platelet disorders; A Trousseau Children Hospital Paris, France

<sup>15</sup>Gustave Roussy Institute, UMR 1170, Villejuif, France

<sup>16</sup>Department of Physiology, Development and Neuroscience, University of Cambridge, Cambridge, CB2 3EG, UK

<sup>17</sup>Department of Haematology and MRC Biostatistics Unit, University of Cambridge, Cambridge, UK

<sup>18</sup>Wellcome Trust Sanger Institute, Wellcome Trust Genome Campus, Hinxton, United Kingdom.

<sup>19</sup>Department of Haematology, University of Cambridge, Cambridge Biomedical Campus, Cambridge, United Kingdom

<sup>20</sup>NHS Blood and Transplant, Cambridge Biomedical Campus, Cambridge, United Kingdom

\*contributed equally

**Corresponding authors:**

Inga Hofmann, MD, Assistant Professor of Pediatrics, University of Wisconsin, Madison, UW Health, WIMR 4151, 1111 Highland Avenue, Madison, WI 53705

Email: [ihofmann@wisc.edu](mailto:ihofmann@wisc.edu)

Phone: (608) 263-6405

Fax: (608) 265-9721

Yotis Senis, PhD, Professor of Cellular Haemostasis, University of Birmingham, Birmingham, UK, B15 2TT

Email: [y.senis@bham.ac.uk](mailto:y.senis@bham.ac.uk)

Phone: +44 (0)121 414 8308

**Word count:**

Abstract: 216

Manuscript: 4480

Figures/Tables: 6/2

Supplemental Figures: 15

Supplemental Material:

References: 50

**Running title:** Congenital Myelofibrosis due to G6b-B Mutations

**Key words:** myelofibrosis, congenital myelofibrosis, familial myelofibrosis, myeloproliferative neoplasm, C6orf25, MPIG6B, G6b-B, megakaryocytes, platelets, thrombocytopenia, transgenic mouse

## Key Points

- Autosomal recessive loss-of-function mutations in G6b-B (*MPIG6B*) cause congenital macrothrombocytopenia with focal myelofibrosis (cMTFM).
- G6b-B has orthologous physiological functions in human and mice regulating megakaryocyte and platelet production and function.

## Abstract

Unlike primary myelofibrosis (PMF) in adults, myelofibrosis in children is rare. Congenital (inherited) forms of myelofibrosis (cMF) have been described, but the underlying genetic mechanisms remain elusive. Here we describe 4 families with autosomal recessive inherited macrothrombocytopenia with focal myelofibrosis due to germline loss-of-function mutations in the megakaryocyte-specific immunoreceptor tyrosine-based inhibitory motif (ITIM)-containing receptor G6b-B (*G6b*, *C6orf25* or *MPIG6B*). Patients presented with a mild-to-moderate bleeding diathesis, macrothrombocytopenia, anemia, leukocytosis and atypical megakaryocytes associated with a distinctive, focal, perimegakaryocytic pattern of bone marrow fibrosis. In addition to identifying the responsible gene, the description of G6b-B as the mutated protein potentially implicates aberrant G6b-B megakaryocytic signaling and activation in the pathogenesis of myelofibrosis. Targeted insertion of human *G6b* in mice rescued the knockout phenotype and a copy number effect of human G6b-B expression was observed. Homozygous knockin mice expressed 25% of human G6b-B and exhibited a marginal reduction in platelet count and mild alterations in platelet function; these phenotypes were more severe in heterozygous mice that expressed only 12% of human G6b-B. This study establishes G6b-B as a critical regulator of platelet homeostasis in humans and mice. In addition, the humanized *G6b* mouse will provide an invaluable tool for further investigating the physiological functions of human G6b-B as well as testing the efficacy of drugs targeting this receptor.

## Introduction

Myelofibrosis in children is rare, and, in children, is most commonly seen in association with acute megakaryoblastic leukemia.<sup>1</sup> Other causes include acute lymphoblastic leukemia (ALL),<sup>2</sup> Hodgkin lymphoma<sup>3</sup>, severe vitamin D or C deficiency,<sup>4,5 6</sup> renal osteodystrophy<sup>7</sup>, osteopetrosis, hyperparathyroidism<sup>8</sup>, autoimmunity,<sup>9-11</sup> and tuberculosis.<sup>12</sup> The clinical, histologic and molecular features of pediatric myelofibrosis differ from primary myelofibrosis (PMF) in adults, which is typically due to somatic gain-of-function mutations in tyrosine kinase (TK) signaling pathways, including *JAK2 V617F* (50%), *MPL W515K/L* (5-10%) or *CALR* (35%);<sup>13,14</sup> TK mutations are not typically present in pediatric myelofibrosis, particularly not in young children.<sup>15,1,16</sup> Children with myelofibrosis have a heterogeneous phenotype with variable outcomes. Some patients have spontaneous resolution,<sup>17,18</sup> while others have an aggressive clinical course with progressive, sometimes fatal disease cured only by hematopoietic stem cell transplantation (HSCT)<sup>15,19-21</sup>.

Congenital or inherited forms of myelofibrosis (cMF) are exceedingly rare with fewer than 50 cases reported.<sup>15,18-26</sup> Many cases occur in consanguineous families,<sup>15,19,25</sup> suggesting that cMF can be inherited as a autosomal recessive Mendelian trait. Genetic lesions have been identified in only a small minority of cases. In some, concurrent single lineage cytopenias have been described. For example, homozygous germline mutations in *VPS45* cause neutropenia, neutrophil dysfunction, bone marrow (BM) fibrosis, progressive marrow failure and organomegaly.<sup>27,28</sup> In some patients, fibrosis coexists with an intrinsic platelet disorder, such as gray platelet syndrome (GPS) to gain-of-function mutations in the Growth Factor Inhibitor 1B (*GFI1B*) gene<sup>29</sup> or biallelic mutations in neurobeachin-like 2 (*NBEAL2*).<sup>30-32</sup> These phenotypes are quite distinct from most patients with cMF.

Here we describe the clinical phenotype, distinctive histological features and biallelic loss-of-function mutations in the megakaryocyte-specific immunoreceptor tyrosine-based inhibitor motif (ITIM)-containing receptor G6b-B (*C6orf25* or *MIPG6B*, referred to as *G6b*) in four families with a clinically distinctive form of cMF associated with macrothrombocytopenia and focal myelofibrosis (cMTFM). These phenotypes closely resemble those reported in *G6b* knockout (*KO*) and loss-of-function mice (*Geer et al. co-submitted*).<sup>33</sup> A humanized *G6b* transgenic knockin (*KI*) mouse model establishes that human and mouse G6b-B perform orthologous functions. Mice homozygous for human *G6b* (*G6b<sup>hu/hu</sup>*) exhibit a mild platelet disorder attributed to reduced human G6b-B expression. Reduced G6b-B expression in *G6b<sup>hu/hu</sup>* and heterozygous (*G6b<sup>hu/-</sup>*) mice also revealed novel regulatory roles of G6b-B with respect to immunoreceptor tyrosine-based activation motif (ITAM) and hemi-ITAM receptor signaling.

## **Materials and Methods**

### **Patients**

Families 1-3 consented to the Pediatric Myelodysplastic Syndrome and Bone Marrow Failure Registry (Boston Children's Hospital, Protocol #10-02-0057). Family 4 was consented to the Biomedical Research Centres/Units Inherited Diseases Genetic Evaluation-Bleeding and Platelet Disorders (BRIDGE-BPD) study (UK REC10/H0304/6). All studies were conducted according to the Declaration of Helsinki.

### **Hematological characterization and sample preparation**

Complete blood counts (CBC) and BM aspirates and biopsies were obtained on all clinically affected individuals; CBCs were obtained on other family members. Whole blood or BM mononuclear cell DNA was extracted using the Qiagen Puregene Blood Kit (Qiagen, Germantown, MD). BM aspirate and biopsy histology were prepared using standard clinical procedures. Images were obtained with an Olympus BX43 microscope and DP25 digital camera and acquired with the Olympus CellSens Entry Imaging Software.

### **Flow cytometry, immunohistochemistry, and immunoblotting**

Flow cytometry was performed on an BD Accuri C6 flow cytometer using methods and antibodies described in the Supplemental Methods. Immunohistochemical (IHC) staining for CD61 was done on Bouin's-fixed, paraffin-embedded tissue sections using the Ventana Discovery XT automated platform. A similar, custom automated IHC method was developed using a monoclonal antibody directed against the N-terminal ectodomain of G6b-B.<sup>33</sup> Western blotting and immunoprecipitations were performed as previously described.<sup>34</sup>

### **Linkage and sequencing analysis**

Affymetrix 6.0 SNP genotyping (QuintilesIMS, Research Triangle Park, NC) was performed on

members of the index family (Family 1) and analyzed using a custom platform (Variant Explorer, K.S.-A. and K.M., unpublished). Whole exome sequencing (WES) was performed in patients and immediate family members of Family 1 using the Illumina TrueSeq enrichment protocol. Families 2 and 3 were sequenced using the Agilent SureSelect exome capture enrichment protocol. Sequencing was performed on an Illumina HiSeq 2000/2500 with 100bp paired-end sequencing with an average depth of 40-200x (Macrogen, Rockville, MD). FASTq sequences were processed and analyzed using the WuXi/NextCode platform (Cambridge, MA). For individual 4-II-3, DNA library preparation, sequencing, variant calling and variant filtering were performed as described previously.<sup>35</sup> Confirmatory Sanger sequencing was carried out on all patients and available family members as described in the Supplementary Methods.

### **Mouse models**

Humanized *G6b KI* mice were generated as outlined in Figure S1 and supplementary material (Taconic Biosciences, Cologne, Germany). *G6b* constitutive *KO* (*G6b*<sup>-/-</sup>) mouse models were generated as previously described.<sup>33</sup> All mice were on a C57BL/6 background and procedures were undertaken with UK Home Office approval, in accordance with the Animals (Scientific Procedures) Act of 1986. Detailed descriptions of all other methods can be found in Supplementary Methods.

## Results

### Clinical and pathological characteristics

We studied four consanguineous Arab families presenting with macrothrombocytopenia, anemia and myelofibrosis. Family 1, from the United Arab Emirates (UAE), had three affected male siblings born to first cousin parents. Affected individuals (Figure 1A and Table 1, 1-III-1, 1-III-5, and 1-III-6) had macrothrombocytopenia with variably reduced platelet granularity, and microcytic anemia. BM studies revealed clusters of atypical megakaryocytes with reticulin fibrosis that was most pronounced in proximity to the megakaryocytes. Affected children had mild to moderate bleeding symptoms and required frequent platelet and occasional red cell transfusions; each affected individual shared a homozygous human leukocyte antigen (HLA) haplotype and had congenital adrenal hyperplasia (CAH) due to 21-hydroxylase (CYP21A2) deficiency. The children had three apparently unaffected cousins born to siblings of their parents. One female cousin had CAH and shared the same homozygous HLA type as her affected cousins (Figure 1A and Table 1, 1-III-9.). She was not thrombocytopenic and had only rare large platelets on her peripheral blood smear (Figure 2C). While being evaluated as a transplant donor for her cousins, she underwent multiple BM studies, the first of which showed several lymphoid aggregates with associated reticulin, but normal megakaryocytes. Follow-up BM studies (Figure 2F, I) were normal. Given the lack of a sibling, unrelated or cord blood donor, persistent transfusion dependency and lack of response to immunomodulatory agents, patients 1-III-5 and 1-III-6 underwent successful matched related HSCTs with 1-III-9 serving as the donor. Both patients engrafted and are doing well following HSCT. The proband in this family, 1-III-1, was transplanted using a haploidentical approach from his mother, and eventually succumbed to transplant-related complications.<sup>15</sup>

Family 2 (Figure 1) is from Saudi Arabia. The proband (2-II-6), whose parents are first cousins, had transient thrombocytopenia at birth. Thrombocytopenia recurred at 6-months of life and was associated with severe microcytic anemia unresponsive to iron therapy. BM studies performed elsewhere at age 2-years were reported to be normal. Severe thrombocytopenia and anemia persisted despite several courses of intravenous immunoglobulin and steroids. A BM at age 3-years showed a hypercellular marrow with increased lymphocytes, and clustering of atypical megakaryocytes with focal reticulin fibrosis. The patient's older brother (2-II-5) was found to be an HLA identical match, but was ineligible as a donor due to moderate macrothrombocytopenia. BM studies are not available for this individual, though he is presumed to be clinically affected. Given the lack of a suitable donor and their mild phenotype requiring only occasional platelet transfusions, both children continue to be monitored.

The proband in Family 3 (Figure 1A, 3-II-4) is the daughter of first cousin consanguineous parents from the UAE. She presented at 15-months of age with leukocytosis, severe microcytic anemia and macrothrombocytopenia. Her clinical features were strikingly similar to the affected children in Family 1. Her BM showed a mildly hypercellular marrow for her age with a relative myeloid hyperplasia and clusters of atypical megakaryocytes with associated reticulin fibrosis. Although Family 1 and Family 3 are not known to be related, 3-II-4 also has CAH and shares the same homozygous HLA type and CYP21A2 mutation as Family 1. She is currently being followed without therapeutic intervention. *JAK2*, *MPL* and *CALR* mutation analysis was negative in patients from Families 1-3 (Table 1).

The fourth family included an affected male and female sibling pair with macrothrombocytopenia, increased BM megakaryocytes, and grade II BM myelofibrosis

(Figure 1A, 4-II-2, 4-II-3). These children and an unaffected brother were born to first cousins of Arab descent. The affected boy (4-II-2) had a more severe phenotype, including anemia with Howell-Jolly bodies, elevated fetal hemoglobin, dyserythropoiesis and dysmegakaryopoiesis. Platelet surface expression of GPIIb/IIIa,  $\alpha$ IIb,  $\alpha$ 2 and GPIV were all unaltered, and there was a minor reduction in aggregation to ADP (*data not shown*).

A detailed description of each case is included in the Supplemental Data.

### **Linkage, mutational and protein expression analyses**

We performed Affymetrix SNP 6.0 genotyping on peripheral blood DNA from 10 individuals from Family 1 and assessed shared regions of homozygosity by descent in 1-III-5 and 1-III-6; 1-III-9 was regarded as having an ambiguous phenotype. The major histocompatibility locus (MHC) on chromosome 6p, which, although not statistically significant, showed the strongest linkage (LOD=2.01, Figure 1B). We focused on this region, because affected individuals in Family 1 and 3 had an identical homozygous HLA type and congenital adrenal hyperplasia (CAH) due to the identical CYP21A2 mutation (Table 1). Furthermore, both affected individuals in Family 2 had a different, but homozygous, HLA haplotype; the CYP21A2 and HLA loci are located at 6p21.33 and 6p21.32-6p22.1, respectively (Figure 1B).

We performed WES on nuclear families 1-3, and on individual 4-II-3 and interrogated the results for genes in which unambiguously affected members of each family carried a homozygous rare variant (allele frequency <0.005) within the candidate disease interval predicted to be functionally deleterious. The only gene meeting these criteria was the megakaryocyte and platelet-specific receptor G6b (*MPIG6B*, *C6orf25*, referred to as *G6b-B* or *G6b*).

G6b-B is a transmembrane receptor expressed on the surface of platelets and megakaryocytes.<sup>33,36-38</sup> G6b-B has one extracellular immunoglobulin-like domain, a single transmembrane domain and an immunoreceptor tyrosine-based inhibitory motif (ITIM) and immunoreceptor tyrosine-based switch motif (ITSM) in its cytoplasmic tail. Tyrosine phosphorylation of the ITIM and ITSM provides a docking site for the SRC homology 2 (SH2) domain-containing tyrosine phosphatases SHP1 (*PTPN6*) and SHP2 (*PTPN11*), which mediate downstream signalling.<sup>39,40</sup> Murine KO and loss-of-function models of *G6b* result in a phenotype very similar to the patients, including macrothrombocytopenia, abnormal platelet function and the perimegakaryocytic pattern of bone marrow fibrosis present in patients (*Geer et al. co-submitted*).<sup>33</sup> BM-derived mouse G6b-B-deficient megakaryocytes develop and proliferate normally *in vitro*, but failed to form highly branched proplatelets, suggesting that G6b-B regulates proplatelet formation, correlating with reduced platelet production.<sup>33</sup>

Families 1 and 3 shared the same variant, a two base pair duplication bridging a splice donor site, NM\_138272.2 c.61\_61+1dup (p.?), and Family 2 had a unique homozygous frameshift mutation, c.149dup (p.Ala52GlyfsX128, Figure 1B). These variants segregated with the phenotype in families 2 and 3; however, in family 1, individual 1-III-9, who had served as the HSCT donor for her cousins, genotyped as a homozygous mutant, despite having no overt clinical features of the disease other than rare giant platelets (Figure 2C). In Family 4, we found a novel apparently homozygous missense variant c.469G>A (p.Gly157Arg, Figure 1B). The variant was also homozygous in the affected brother.

Residues 143-163 encode the predicted transmembrane domain of G6b-B, and substituting a glycine with arginine would likely destabilize insertion of the receptor into the membrane. Expression of the p.Gly157Arg mutant protein was tested using transiently transfected DT40

cells. Introduction of the mutation caused a significant reduction in total G6b-B protein expression (Figure 1C), and surface expression was reduced by 84% by flow cytometry (Figures 1D, E). A comparable reduction in expression was also observed in transiently transfected Chinese hamster ovary (CHO) cell line (*data not shown*). These data suggest that this rare missense variant is functionally significant.

To further validate *G6b* variants as disease-causing, we evaluated G6b-B expression in BM biopsy specimens from affected patients and control samples by IHC using a monoclonal antibody specific to the ectodomain. G6b-B was strongly and selectively expressed in megakaryocytes and platelets of control BM samples, but completely absent in megakaryocytes and platelets of the genotypically affected individuals from families 1-3 (Figure 2J-2O). BM biopsy samples were not available for patient 4-II-2 or 4-II-3 with the p.Gly157Arg mutation. Thus, in combination with the complementary phenotype observed in *G6b*<sup>-/-</sup> mice,<sup>33</sup> the thrombocytopenia and BM myelofibrosis found in these patients is almost certainly due to reduced or absent expression of G6b-B.

### **Expression of human G6b-B in *G6b*<sup>hu/hu</sup> mice**

To confirm that human and mouse G6b-B are orthologous, we generated a humanized *G6b* mouse model in which mouse *G6b* was replaced with its human counterpart (Figure S1 and Supplemental Methods). Mice were born at expected Mendelian frequencies from heterozygous (*G6b*<sup>hu/+</sup>) breeding pairs (Table S1), and *G6b*<sup>hu/hu</sup> mice were healthy, fertile and survived >25 weeks without any overt developmental or growth anomalies. Expression of human and mouse G6b-B was verified by flow cytometry (Figure S2) and western blotting (Figure 3A). Expression of the human G6b-A splice isoform, which lacks the ITIM and ITSM,

was also demonstrated using an isoform-specific antibody (Figure 3Ai, iv). Both human isoforms were only expressed at 25% of normal human platelet levels. The ratio of glycosylated (32 kDa) to unglycosylated (28 kDa) human G6b-B and -A was reduced from 3:2 in human platelets to 2:3 in *G6b<sup>hu/hu</sup>* platelets (Figure 3B).

The ability of human G6b-B to bind mouse Shp1 and Shp2 was also investigated in *G6b<sup>hu/hu</sup>* platelets (Figure 3C). Similar amounts of human and mouse Shp1 and Shp2 co-immunoprecipitated (co-IP'd) with human G6b-B from human and *G6b<sup>hu/hu</sup>* platelets under resting conditions (Figure 3Cii). However, less Shp1 co-IP'd with human G6b-B from *G6b<sup>hu/hu</sup>* platelets compared with human platelets following collagen-stimulation, most likely reflecting differences in expression levels of Shp1 and Shp2 in human and mouse platelets (Figure S3).<sup>41,42</sup> In contrast, comparable amounts of Shp2 co-IP'd with human G6b-B from collagen-stimulated human and *G6b<sup>hu/hu</sup>* platelets.

### **Human G6b-B functionally replaces mouse G6b-B**

Reduced human G6b-B expression resulted in an 21% reduction in platelet count and a marginal increase in platelet volume in *G6b<sup>hu/hu</sup>* mice (Table 2, Figure S4). In contrast, complete ablation of *G6b* resulted in a >80% reduction in platelet count and >30% increase in platelet volume (Table 2), demonstrating that human G6b-B rescues the *KO* phenotype. Altered blood cell counts in *G6b KO* mice were independent of age (Figure S5). Histological sections of spleens and femurs also demonstrated that expression of human *G6b* rescues the perimegakaryocytic pattern of bone marrow fibrosis previously identified in *G6b KO* mice (Figure S6).<sup>33</sup> All other hematological parameters were normal in *G6b<sup>hu/hu</sup>* mice (Table 2).

Blood counts were normal in  $G6b^{+/hu}$  and  $G6b^{+/-}$  mice (Table 2).<sup>33</sup> Platelet surface levels of GPVI, CLEC-2,  $\alpha 2$ ,  $\alpha IIb$  and GPIb $\alpha$  were normal in platelets from  $G6b^{hu/hu}$  mice (Figure S7).

### Reduced human G6b-B expression causes minor alterations in platelet function

$G6b^{hu/hu}$  platelets provide a unique model to investigate the physiological consequence of reduced human G6b-B levels in platelets, without altered expression of other receptors identified in  $G6b^{-/-}$  mice.<sup>33</sup> No significant defects were observed in  $\alpha IIb\beta 3$ -mediated adhesion and spreading of  $G6b^{hu/hu}$  platelets on fibrinogen, in the presence or absence of thrombin (Figure S8). Consistent with these findings, outside-in  $\alpha IIb\beta 3$  signaling was comparable between *WT* and  $G6b^{hu/hu}$  platelets (Figure S9). Bands corresponding to tyrosine phosphorylated mouse (45 kDa) and human (28-34 kDa doublet) G6b-B were observed in fibrinogen-adhered *WT* and  $G6b^{hu/hu}$  platelets, respectively. As  $G6b^{hu/hu}$  mice do not express mouse G6b-B (Figure 3), the tyrosine phosphorylated band at 45 kDa is due to the presence of other co-migrating phosphorylated proteins.

We next investigated (hemi)-ITAM receptor-mediated functional responses. Unexpectedly, platelet aggregation was marginally reduced in response to low and intermediate concentrations (1-10  $\mu\text{g/ml}$ ) of the GPVI-specific agonist collagen-related peptide (CRP) (Figure 4A). In contrast, CLEC-2-mediated platelet aggregation was marginally increased at 6  $\mu\text{g/ml}$  anti-CLEC-2 antibody (Figure 4A). Platelet aggregation to thrombin, collagen, ADP and the TxA<sub>2</sub> analogue U46619 were normal (Figure S10). ATP secretion from dense granules was normal to all agonists tested (Figure 4A and S10), except for a minor increase at an intermediate dose of collagen. These findings reveal minor alternations in platelet functional

responses due to reduced human G6b-B expression that are likely of no physiological consequence.

### **Altered $G6b^{hu/hu}$ platelet function does not affect thrombus formation or hemostasis**

We further investigated  $G6b^{hu/hu}$  platelet functional responses under physiological flow conditions on different thrombogenic surfaces. Platelet adhesion and thrombus formation were quantified by flowing anti-coagulated blood over: (1) collagen; (2) von Willebrand Factor-binding protein (vWF-BP) and laminin; and (3) vWF-BP, laminin and the CLEC-2 agonist rhodocytin, for 3.5 minutes at  $1,000\text{ s}^{-1}$ . Surface area coverage and morphological scores were used as measures of platelet adhesion and thrombus formation (Figure S11). Regression analysis of a cohort of *WT* mice ( $n=19$ ) did not indicate that the 21% reduction in platelet counts in  $G6b^{hu/hu}$  mice will affect any of the measured parameters (Figure S12). The total surface area covered by  $G6b^{hu/hu}$  platelets on collagen was unaltered compared with *WT* platelets (Figure 4B). However, multilayer thrombus formation and contraction were both significantly increased, despite a minor reduction in  $\alpha\text{IIb}\beta\text{3}$  activation and normal  $\alpha$ -granule release, measured by immunostaining with JON/A and P-selectin antibodies, respectively (Figure 4B). Altered thrombus morphology of  $G6b^{hu/hu}$  platelets is most likely a reflection of the increased proportion of phosphatidylserine (PS)-positive procoagulant platelets, measured by Annexin V staining (Figure 4B).

No difference in adhesion or platelet activation were observed when anti-coagulated blood from *WT* and  $G6b^{hu/hu}$  mice was flowed over vWF-BP and laminin, or vWF-BP, laminin and rhodocytin (Figure S13). Although some minor alterations in  $G6b^{hu/hu}$  platelet activation were identified using this assay, expression of human G6b-B rescued the severe defects observed

in  $G6b^{-/-}$  platelets. This rescue is likely due to a combination of increased platelet counts and normalized platelet reactivity. Functional defects observed in  $G6b^{hu/hu}$  platelets did not culminate in compromised hemostasis in mice, as assessed using the tail bleeding assay, whereas  $G6b^{-/-}$  mice bled excessively, as previously reported (Figure 4C).<sup>33</sup>

To determine the molecular basis of altered responses to CRP and anti-CLEC-2 antibody, we investigated tyrosine phosphorylation in  $WT$  and  $G6b^{hu/hu}$  platelets. The findings from aggregations studies were supported by a minor reduction in global tyrosine phosphorylation following CRP stimulation (Figure 5A). A trend towards reduced SFK and Syk activities was identified, as measured by changes in autophosphorylation of Tyr418 and Tyr519/20 in the activation loops of SFKs and Syk, respectively, though this did not reach significance (Figure 5A). SFK-mediated phosphorylation of the ITAM-containing FcR  $\gamma$ -chain, which acts as a docking site for Syk to propagate signals downstream of GPVI, was also marginally reduced in CRP-stimulated  $G6b^{hu/hu}$  platelets. The opposite was observed in CLEC-2 activated platelets, in which global tyrosine phosphorylation, SFK and Syk activation were marginally increased in response to antibody-mediated cross-linking and activation of CLEC-2 (Figure 5B). However, only Syk activation with 10  $\mu$ g/ml anti-CLEC-2 antibody was significantly increased.

### **Further reduction in human G6b-B expression exacerbates platelet defects**

To further investigate the threshold of human G6b-B expression required to rescue the  $G6b^{-/-}$  phenotype, we generated human  $G6b$  hemizygous mice ( $G6b^{hu/-}$ ) by crossing  $G6b^{hu/hu}$  mice with  $G6b^{-/-}$  mice (Figure 6A).  $G6b^{hu/-}$  mice expressed only 12% of human G6b-B and -A compared with human platelets, and no mouse G6b-B (Figure 6A and S14A, B). These expression levels produced an even greater reduction in platelet counts (29%) and a

comparable increase in platelet volume (6-7%) compared with  $G6b^{hu/hu}$  mice (Table 2). This provides further evidence that human G6b-B dose dependently regulates platelet production. Surface receptor expression was normal in  $G6b^{hu/-}$  platelets compared with *WT* platelets, except for CLEC-2, which was marginally reduced by 16% (Figure S14C). Interestingly, platelet aggregation was further reduced in response to CRP and increased in response to antibody-mediated cross-linking of CLEC-2 (Figure 6B). These findings demonstrate differential roles of G6b-B in regulating ITAM- and hemi-ITAM-containing receptor-mediated platelet activation at these expression levels. No difference was observed upon activation of CLEC-2 using the snake toxin rhodocytin. This likely reflects the tetravalent structure of rhodocytin that can elicit a more robust CLEC-2 activating signal, thus abrogating the mild phenotype observed with the bivalent anti-CLEC-2 antibody. Thrombin-mediated aggregation of  $G6b^{hu/-}$  platelets was normal and no significant defects in ATP secretion was observed for all agonists tested.

## Discussion

Here we have described four families with a distinct phenotype of macrothrombocytopenia, microcytic anemia, variable leukocytosis and histologically characteristic megakaryocytic clustering, dysplasia and focal reticulin fibrosis in the BM presenting at young age. We attribute this to homozygous loss-of-function mutations in *G6b*, the gene encoding G6b-B, a megakaryocytic/platelet-specific ITIM-containing receptor. While this work was in preparation, another consanguineous Arab family with a similar phenotype was described with a homozygous predicted null mutation in *G6b*.<sup>26</sup> These data firmly support the conclusion that recessive loss-of-function mutations in *G6b* result in the phenotype that we comprehensively describe and term congenital macrothrombocytopenia with cMTFM. All of the clinically affected patients have a phenotype strikingly similar to a null mutation,<sup>33</sup> or mutations that abolish ITIM/ITSM signaling, (*Geer et al. co-submitted*) in the murine orthologue. Concomitantly, we have demonstrated that the *G6b* KO phenotype can be rescued upon expression of human *G6b*.

One apparently clinically unaffected individual, 1-III-9, without thrombocytopenia or anemia at the time of her evaluation as a transplant donor, also shares the G6b-B mutation; she did not have thrombocytopenia, bleeding symptoms, leukocytosis, anemia, or atypical megakaryocytes associated with fibrosis, but did have rare large platelets. She did have transient BM lymphoid aggregates that are unusual for such a young child; these might be indicators of a primary BM disorder, but could equally be due to her CAH or other causes. Thus, it is likely that even genotypically similar patients might have varying expressivity or penetrance of the phenotype due to other modifying factors, including age, environment, and genotypes at other loci. Indeed, for example, patient 2-II-5 came to medical attention only

because of his more severely affected younger sibling, 2-II-6. In addition to modifiers noted above, there are several possible explanations for the successful HSCT of the two siblings, 1-III-5 and 1-III-6 from their cousin, 1-III-9, who shares the same homozygous mutant *G6b* genotype. First, it is conceivable that the conditioning regimen alters the niche directly, which could impact the regulation of other components important in the regulation of megakaryocytic development, proplatelet and platelet formation. Second, introduction of a new hematopoietic stem cell pool from the donor into the host with cMF could lead to immunological graft and host interactions between the stem cell compartment and the niche that could alter megakaryocytic development.

The cMTFM phenotype underscores the importance of G6b-B signaling in normal megakaryocyte and platelet biology. Binding of Shp1 and Shp2 are essential for mediating signal transduced by G6b-B. A mutant form of G6b-B that uncouples it from Shp1 and Shp2 signaling phenocopies the *G6b* KO mouse model (*Geer et al. co-submitted*),<sup>33</sup> and a tissue-specific mouse model of combined Shp1 and Shp2 deficiency recapitulates multiple features of *G6b* KO animals,<sup>43</sup> further indicating the essential nature of this signaling pathway to megakaryocyte function.

The majority of reported patients with cMF have undergone HSCT as it was felt to be the only curative treatment option.<sup>15</sup> The histological resemblance to PMF in adults, which carries a risk of evolution to acute myeloid leukemia and a poor prognosis, may have encouraged providers to offer HSCT out of due caution, even in the absence of evidence for adverse outcomes when managed conservatively. Indeed, in our series of 7 cases of patients with *G6b* mutations, three required HSCT for cytopenias, one was clinically unaffected, and three have been observed without ongoing clinical interventions. The identification of a molecular therapeutic

target—Shp1- and Shp2-dependent signal transduction—now offers the potential to circumvent the G6b-B deficiency in cMTFM and insights into the pathogenesis of other forms of primary and secondary myelofibrosis.

The humanized *G6b* mouse provided compelling evidence of the analogous functions of human and mouse G6b-B. The mild platelet phenotype, suggests human G6b-B interacts with the same ligands and signals in a similar manner to mouse G6b-B. Reduced binding of human G6b-B to mouse Shp1 is most likely a reflection of the relative stoichiometries and binding affinities of Shp1 and Shp2 in mouse platelets. Mouse platelets contain 6-fold higher levels of Shp2 than Shp1, whereas human platelets contain 2-fold more Shp1 than Shp2 (Figure S3).<sup>41,42</sup> In addition, the binding affinity of tandem SH2 domains of human Shp2 with phosphorylated-G6b-B-ITIM-ITSM peptide is 100-fold greater than the binding affinity of tandem SH2 domains of Shp1.<sup>44</sup> However, differences in the proportions of human G6b-B bound Shp1 and Shp2 in mouse versus human platelets are not likely to underlie the platelet defects described the humanized *G6b* mouse, as mouse G6b-B is predicted to bind the same ratios of Shp1 and Shp2. Thus, platelet defects are more likely due to reduced human G6b-B expression.

Despite the significant reduction in human G6b-B in *G6b<sup>hu/hu</sup>* and *G6b<sup>hu/-</sup>* mice, both mouse models exhibited only mild platelet phenotypes. A large proportion of G6b-B is therefore not essential for maintenance of platelet homeostasis. MKs from *G6b<sup>-/-</sup>* mice were previously shown to develop normally *in vitro*, but with significantly diminished proplatelet production capacity.<sup>33</sup> Reduced platelet production in *G6b<sup>hu/hu</sup>* and *G6b<sup>hu/-</sup>* mice could therefore have been as a consequence of aberrant proplatelet formation, arising from reduced G6b-B expression in MKs. The dose dependent nature of the reduction in platelet counts in these

homozygous and heterozygous mice adds to the growing body of evidence of the vital role of G6b-B in regulating platelet production.

The reduction in human G6b-B expression was predicted to lead to an increase in platelet reactivity to collagen. Indeed, thrombus formation and contraction were significantly increased when whole blood was flowed over collagen, despite a marginal reduction in integrin  $\alpha$ IIb $\beta$ 3 activation. This can be explained by an enhancement in PS exposure and increased procoagulant activity of *G6b<sup>hu/hu</sup>* platelets, which is dependent upon PLC $\gamma$ 2-mediated Ca<sup>2+</sup> flux and phosphatidylinositol 3-kinase signaling,<sup>45</sup> highlighting these as potential downstream targets of Shp1 and Shp2. The dose-dependent reduction in aggregation of *G6b<sup>hu/hu</sup>* and *G6b<sup>hu/-</sup>* platelets to CRP was however, counter-intuitive, suggesting G6b-B may act as both a positive and negative regulator of GPVI signaling, depending upon expression levels. The candidate target of G6b-B-associated Shp1 and Shp2 is Syk tyrosine kinase that we previously showed is hyper-activated in G6b-B-deficient platelets.<sup>33</sup> Syk contains multiple regulatory tyrosine phosphorylation sites that Shp1 and Shp2 may differentially dephosphorylate, depending upon the expression level of G6b-B, leading to either positive or negative effects on Syk activity.<sup>46</sup>

This study establishes that human and mouse G6b-B perform the same physiological functions, and that deletion and loss-of-function mutations in G6b-B lead to megakaryocytic and myelofibrotic disorders in both species. Validation of these analogous functions is essential to progress with exploring the role of G6b-B in various pathological conditions in humans and as a novel therapeutic drug target. The humanized G6b-B mouse model described here provides an invaluable tool for investigating the efficacy and therapeutic potential of agents targeting human G6b-B in various disease conditions, including

myeloproliferation and myelofibrosis, allowing for a greater understanding of the mechanism of action of these therapies.

### **Acknowledgements**

Sample collection and clinical and pathology analysis was performed under the Pediatric MDS and BMF Registry supported by NIH grant R24 DK 099808. I.H. and M.D.F. are supported by R24 DK099808. M.J.G. is funded by a Medical Research Council PhD studentship (GBT1564), A.M. is a BHF Intermediate Basic Science Research Fellow (FS/15/58/31784) and Y.A.S. is a BHF Senior Basic Science Research Fellow (FS/13/1/29894). T.V. was funded by the Deutsche Forschungsgemeinschaft (DFG V2134-1/1).

### **Authorship Contributions**

I.H. – identified patients, analyzed the clinical and pathologic phenotypes, designed the study, wrote and revised the manuscript

M.J.G. – performed experiments, analyzed data, wrote and revised the manuscript

T.V. – performed experiments, analyzed data, revised the manuscript

A.C. – performed patient sample processing and sequencing analysis

D.R.C. – performed patient sample processing and sequencing analysis

A.B. – performed experiments, analyzed data

M.L.C. – developed the customized immunohistochemistry for G6b-B

S.H. – performed experiments, analyzed data

J.P.V.G. – performed experiments, analyzed data, revised the manuscript

M.J.E.K. – performed experiments, analyzed data

J.W.M.H. – performed experiments, analyzed data

J.A.E. – provided snake toxin rhodocytin

K.S.A. – performed linkage and WES data analysis

E.A.O. – provided patient care

M.D. – performed experiments, analyzed data

K.F. – performed GWAS

C.P. – identified and diagnosed patient

R.F. – identified and diagnosed patient

G.E.J. – analyzed data, revised the manuscript

K.M. – performed linkage and WES data analysis

E.T. – analyzed data, revised the manuscript

W.H.O. – analyzed data, contributed intellectually

A.M. – designed experiments, analyzed data, revised the manuscript

M.D.F. – analyzed the clinical and pathologic phenotypes, designed the study, wrote and revised the manuscript

Y.A.S. – conceptualized, designed experiments, analyzed data, wrote and revised the manuscript

All authors contributed to the revision of the manuscript.

### **Disclosure of Conflicts of Interest**

The authors have no competing financial interests to declare.

## References

1. Hofmann I. Myeloproliferative Neoplasms in Children. *J Hematop.* 2015;8(3):143-157.
2. Hann IM, Evans DI, Marsden HB, Jones PM, Palmer MK. Bone marrow fibrosis in acute lymphoblastic leukaemia of childhood. *J Clin Pathol.* 1978;31(4):313-315.
3. Carroll WL, Berberich FR, Glader BE. Pancytopenia with myelofibrosis. An unusual presentation of childhood Hodgkin's disease. *Clin Pediatr (Phila).* 1986;25(2):106-108.
4. Balkan C, Ersoy B, Nese N. Myelofibrosis associated with severe vitamin D deficiency rickets. *J Int Med Res.* 2005;33(3):356-359.
5. al-Eissa YA, al-Mashhadani SA. Myelofibrosis in severe combined immunodeficiency due to vitamin D deficiency rickets. *Acta Haematol.* 1994;92(3):160-163.
6. Fain O, Mathieu E, Thomas M. Scurvy in patients with cancer. *BMJ.* 1998;316(7145):1661-1662.
7. Schlackman N, Green AA, Naiman JL. Myelofibrosis in children with chronic renal insufficiency. *J Pediatr.* 1975;87(5):720-724.
8. Kumbasar B, Taylan I, Kazancioglu R, Agan M, Yenigun M, Sar F. Myelofibrosis secondary to hyperparathyroidism. *Exp Clin Endocrinol Diabetes.* 2004;112(3):127-130.
9. Phebus CK, Penchansky L. Autoimmune pancytopenia progressing to acute myelofibrosis. *Scand J Haematol.* 1986;36(3):317-318.
10. Passamonti F, Rumi E, Arcaini L, et al. Prognostic factors for thrombosis, myelofibrosis, and leukemia in essential thrombocythemia: a study of 605 patients. *Haematologica.* 2008;93(11):1645-1651.
11. Paquette RL, Meshkinpour A, Rosen PJ. Autoimmune myelofibrosis. A steroid-responsive cause of bone marrow fibrosis associated with systemic lupus erythematosus. *Medicine (Baltimore).* 1994;73(3):145-152.
12. Hashim MS, Kordofani AY, el Dabi MA. Tuberculosis and myelofibrosis in children: a report. *Ann Trop Paediatr.* 1997;17(1):61-65.
13. Nangalia J, Massie CE, Baxter EJ, et al. Somatic CALR mutations in myeloproliferative neoplasms with nonmutated JAK2. *N Engl J Med.* 2013;369(25):2391-2405.
14. Klampfl T, Gisslinger H, Harutyunyan AS, et al. Somatic mutations of calreticulin in myeloproliferative neoplasms. *N Engl J Med.* 2013;369(25):2379-2390.
15. DeLario MR, Sheehan AM, Ataya R, et al. Clinical, histopathologic, and genetic features of pediatric primary myelofibrosis--an entity different from adults. *Am J Hematol.* 2012;87(5):461-464.
16. An W, Wan Y, Guo Y, et al. CALR mutation screening in pediatric primary myelofibrosis. *Pediatr Blood Cancer.* 2014;61(12):2256-2262.
17. Lau SO, Ramsay NK, Smith CM, 2nd, McKenna R, Kersey JH. Spontaneous resolution of severe childhood myelofibrosis. *J Pediatr.* 1981;98(4):585-588.
18. Altura RA, Head DR, Wang WC. Long-term survival of infants with idiopathic myelofibrosis. *Br J Haematol.* 2000;109(2):459-462.
19. Sieff CA, Malleson P. Familial myelofibrosis. *Arch Dis Child.* 1980;55(11):888-893.
20. Sekhar M, Prentice HG, Popat U, et al. Idiopathic myelofibrosis in children. *Br J Haematol.* 1996;93(2):394-397.
21. Domm J, Calder C, Manes B, Crossno C, Correa H, Frangoul H. Unrelated stem cell transplant for infantile idiopathic myelofibrosis. *Pediatr Blood Cancer.* 2009;52(7):893-895.
22. Boxer LA, Camitta BM, Berenberg W, Fanning JP. Myelofibrosis-myeloid metaplasia in childhood. *Pediatrics.* 1975;55(6):861-865.
23. Mallouh AA, Sa'di AR. Agnogenic myeloid metaplasia in children. *Am J Dis Child.* 1992;146(8):965-967.
24. Sah A, Minford A, Parapia LA. Spontaneous remission of juvenile idiopathic myelofibrosis. *Br J Haematol.* 2001;112(4):1083.
25. Sheikha A. Fatal familial infantile myelofibrosis. *J Pediatr Hematol Oncol.* 2004;26(3):164-168.
26. Melhem M, Abu-Farha M, Antony D, et al. Novel G6B gene variant causes familial autosomal recessive thrombocytopenia and anemia. *Eur J Haematol.* 2017;98(3):218-227.
27. Stepensky P, Saada A, Cowan M, et al. The Thr224Asn mutation in the VPS45 gene is associated with the congenital neutropenia and primary myelofibrosis of infancy. *Blood.* 2013;121(25):5078-5087.
28. Vilboux T, Lev A, Malicdan MC, et al. A congenital neutrophil defect syndrome associated with mutations in VPS45. *N Engl J Med.* 2013;369(1):54-65.
29. Monteferrario D, Bolar NA, Marneth AE, et al. A dominant-negative GFI1B mutation in the gray platelet syndrome. *N Engl J Med.* 2014;370(3):245-253.

30. Albers CA, Cvejic A, Favier R, et al. Exome sequencing identifies NBEAL2 as the causative gene for gray platelet syndrome. *Nat Genet.* 2011;43(8):735-737.
31. Gunay-Aygun M, Falik-Zaccari TC, Vilboux T, et al. NBEAL2 is mutated in gray platelet syndrome and is required for biogenesis of platelet alpha-granules. *Nat Genet.* 2011;43(8):732-734.
32. Kahr WH, Hinckley J, Li L, et al. Mutations in NBEAL2, encoding a BEACH protein, cause gray platelet syndrome. *Nat Genet.* 2011;43(8):738-740.
33. Mazharian A, Wang YJ, Mori J, et al. Mice lacking the ITIM-containing receptor G6b-B exhibit macrothrombocytopenia and aberrant platelet function. *Sci Signal.* 2012;5(248):ra78.
34. Pearce AC, Senis YA, Billadeau DD, Turner M, Watson SP, Vigorito E. Vav1 and vav3 have critical but redundant roles in mediating platelet activation by collagen. *J Biol Chem.* 2004;279(52):53955-53962.
35. Westbury SK, Turro E, Greene D, et al. Human phenotype ontology annotation and cluster analysis to unravel genetic defects in 707 cases with unexplained bleeding and platelet disorders. *Genome Med.* 2015;7(1):36.
36. Lewandowski U, Wortelkamp S, Lohrig K, et al. Platelet membrane proteomics: a novel repository for functional research. *Blood.* 2009;114(1):e10-19.
37. Macaulay IC, Tijssen MR, Thijssen-Timmer DC, et al. Comparative gene expression profiling of in vitro differentiated megakaryocytes and erythroblasts identifies novel activatory and inhibitory platelet membrane proteins. *Blood.* 2007;109(8):3260-3269.
38. Senis YA, Tomlinson MG, Garcia A, et al. A comprehensive proteomics and genomics analysis reveals novel transmembrane proteins in human platelets and mouse megakaryocytes including G6b-B, a novel immunoreceptor tyrosine-based inhibitory motif protein. *Mol Cell Proteomics.* 2007;6(3):548-564.
39. Daeron M, Jaeger S, Du Pasquier L, Vivier E. Immunoreceptor tyrosine-based inhibition motifs: a quest in the past and future. *Immunol Rev.* 2008;224:11-43.
40. Coxon CH, Geer MJ, Senis YA. ITIM receptors: more than just inhibitors of platelet activation. *Blood.* 2017;129(26):3407-3418.
41. Burkhardt JM, Vaudel M, Gambaryan S, et al. The first comprehensive and quantitative analysis of human platelet protein composition allows the comparative analysis of structural and functional pathways. *Blood.* 2012;120(15):e73-82.
42. Zeiler M, Moser M, Mann M. Copy number analysis of the murine platelet proteome spanning the complete abundance range. *Mol Cell Proteomics.* 2014;13(12):3435-3445.
43. Mazharian A, Mori J, Wang YJ, et al. Megakaryocyte-specific deletion of the protein-tyrosine phosphatases Shp1 and Shp2 causes abnormal megakaryocyte development, platelet production, and function. *Blood.* 2013;121(20):4205-4220.
44. Coxon CH, Sadler AJ, Huo J, Campbell RD. An investigation of hierarchical protein recruitment to the inhibitory platelet receptor, G6B-b. *PLoS One.* 2012;7(11):e49543.
45. Munnix IC, Cosemans JM, Auger JM, Heemskerk JW. Platelet response heterogeneity in thrombus formation. *Thromb Haemost.* 2009;102(6):1149-1156.
46. Mocsai A, Ruland J, Tybulewicz VL. The SYK tyrosine kinase: a crucial player in diverse biological functions. *Nat Rev Immunol.* 2010;10(6):387-402.
47. McCarty OJ, Larson MK, Auger JM, et al. Rac1 is essential for platelet lamellipodia formation and aggregate stability under flow. *J Biol Chem.* 2005;280(47):39474-39484.
48. Senis YA, Tomlinson MG, Ellison S, et al. The tyrosine phosphatase CD148 is an essential positive regulator of platelet activation and thrombosis. *Blood.* 2009;113(20):4942-4954.
49. Ohlmann P, Eckly A, Freund M, Cazenave JP, Offermanns S, Gachet C. ADP induces partial platelet aggregation without shape change and potentiates collagen-induced aggregation in the absence of Galphaq. *Blood.* 2000;96(6):2134-2139.
50. de Witt SM, Swieringa F, Cavill R, et al. Identification of platelet function defects by multi-parameter assessment of thrombus formation. *Nature Communications.* 2014;5.

## Tables

**Table 1. Clinical and laboratory characteristics, treatments and outcomes of patients with congenital myelofibrosis.**

ID	Age	Sex	WBC	HGB	PLT	MCV	MPV	Peripheral blood smear morphology	Other clinical features	JAK2	MPL	CALR	Therapy and response	HLA				G6B genotype	Outcome		
														A	B	C	DRB1				
1-III-1	5 m	M	NA	6.0	20	66.0	NA	microcytosis, anisopoikilocytosis, target cells, ovalocytes, large platelets	CAH	Neg	ND	ND	no pre-HSCT therapy S/P 2 haploidentical HSCT from mother	11:01 11:01	41:01 41:01	07:01 07:01	08:04 08:04	03:01 03:01	c.61_61+1dup/ c.61_61+1dup	Deceased from SCT complications, graft failure after 2 <sup>nd</sup> HSCT, GI bleed, ARDS	
1-III-5	Birth	M	NA	6.9	16	NA	NA	anisopoikilocytosis, target cells, basophilic stippling, large platelets	CAH	Neg	Neg	Neg	steroids, transient partial response but not sustained. Platelets declined with taper. MRD HSCT from 1-III-9	11:01 11:01	41:01 41:01	07:01 07:01	08:04 08:04	03:01 03:01	c.61_61+1dup/ c.61_61+1dup	6 years post-HSCT, engrafted, maturing trilineage hematopoiesis with no evidence of fibrosis.	
1-III-6	6 m	M	13.79	8.7	19	68.0	NA	microcytosis, anisopoikilocytosis, target cells, basophilic stippling, tear drops, frequent large platelets	CAH	Neg	Neg	Neg	no pre-HSCT therapy. MRD HSCT from 1-III-9	11:01 11:01	41:01 41:01	07:01 07:01	08:04 08:04	03:01 03:01	c.61_61+1dup/ c.61_61+1dup	4 years post-HSCT. Slow platelet and RBC engraftment. Maturing trilineage hematopoiesis and no evidence of fibrosis, but platelets remain decreased, ~119-142 x10 <sup>9</sup> /L.	
1-III-9	2 y	F	8.39	11.9	468	72.0	8.2	microcytosis	CAH, mild iron deficiency	ND	ND	ND	none	11:01 11:01	41:01 41:01	07:01 07:01	08:04 08:04	03:01 03:01	c.61_61+1dup/ c.61_61+1dup	Clinically unaffected, rare giant platelets	
2-II-5	7 y	M	5.43	11.7	107	80.5	NA	anisopoikilocytosis, microcytosis, ovalocytes, burr cells, helmet cells, acanthocytes, schistocytes, frequent large platelets	None	ND	ND	ND	none	23:01 23:01	50:01 50:01	06:02 06:02	04:06 04:06	04:02 04:02	c.147insT p.Ala52GlyfsX128	Observation, stable disease	
2-II-6	6 m	M	NA	5.4	10	65.0	12-24	anisopoikilocytosis, microcytosis, elliptocytes, schistocytes, frequent large platelets	None	Neg	Neg	Neg	IVIG x1 Steroids x1 with transient responses	23:01 23:01	50:01 50:01	06:02 06:02	04:06 04:06	04:02 04:02	c.147insT p.Ala52GlyfsX128	Observation, stable disease	
3-II-4	17 m	F	19.2	5.1	81	71.3	NA	anisopoikilocytosis, microcytosis, target cells, ovalocytes, burr cells, tear drop cells, schistocytes, frequent large platelets	CAH, asplenia	Neg	Neg	Neg	none	11:01 11:01	41:01 41:01	07:01 07:01	08:04 08:04	03:01 03:01	c.61_61+1dup/ c.61_61+1dup	Observation, stable disease	
4-II-2	18 m	M	NA	5.4	96	NA	NA	Anisopoikilocytosis, target cells, schistocytes, leptocytes, dacryocytes, Howell-Jolly bodies	cerebral cavernoma	ND	Neg	ND	IVIG and steroid, no response	ND	ND	ND	ND	ND	ND	c.469G>A p.Gly157Arg	Observation, stable thrombocytopenia, supportive care with platelets
4-II-3	1 y	F	17	12.5	97	NA	NA	Anisopoikilocytosis, target cells, schistocytes, leptocytes, dacryocytes, Howell-Jolly bodies	None	ND	ND	ND	none	ND	ND	ND	ND	ND	ND	c.469G>A p.Gly157Arg	Observation, stable mild/moderate thrombocytopenia

not available (NA), not done (ND), congenital adrenal hyperplasia (CAH), hematopoietic stem cell transplant (HSCT)

**Table 2. Peripheral blood counts of indicated mouse genotypes**

Hematological parameters	<i>WT</i> n=36	<i>G6b<sup>+/hu</sup></i> n=37	<i>G6b<sup>hu/hu</sup></i> n=37	<i>G6b<sup>hu/-</sup></i> n=31	<i>G6b<sup>-/-</sup></i> n=37	$\lambda$	<i>P</i>
<b>Platelets (10<sup>9</sup>/L)</b>	1118 ± 209	1127 ± 219	884 ± 214***	795 ± 187***	206 ± 86***	0.2	2 × 10 <sup>-72</sup>
<b>Mean platelet volume (fl)</b>	5.8 ± 0.2	5.8 ± 0.2	6.1 ± 0.5***	6.2 ± 0.4***	7.8 ± 0.4***	-2	2 × 10 <sup>-65</sup>
<b>Plateletcrit (%)</b>	0.4 ± 0.1	0.4 ± 0.1	0.3 ± 0.1	0.3 ± 0.1	0.1 ± 0	-	-
<b>Red blood cells (10<sup>12</sup>/L)</b>	11.1 ± 0.7	10.5 ± 0.7	10.7 ± 0.8	10.4 ± 0.6	10.0 ± 0.6	-	-
<b>Hematocrit (%)</b>	33.6 ± 2.4	32.7 ± 1.8	33.1 ± 2.5	34.1 ± 1.9	31.8 ± 1.7	-	-
<b>White blood cells (10<sup>9</sup>/L)</b>	7.5 ± 3.6	8.6 ± 2.3	7.4 ± 2.6	10.1 ± 6.1	13.1 ± 6.8***	0.5	8 × 10 <sup>-7</sup>
<b>Lymphocytes (10<sup>9</sup>/L)</b>	6.2 ± 2.7	7.4 ± 2.0	6.9 ± 2.2	7.8 ± 3.7	11.8 ± 4.9***	0.5	3 × 10 <sup>-11</sup>
<b>Monocytes (10<sup>9</sup>/L)</b>	0.5 ± 0.4	0.3 ± 0.2	0.5 ± 0.2	0.3 ± 0.3	0.5 ± 0.4	-	-
<b>Neutrophils (10<sup>9</sup>/L)</b>	0.8 ± 0.4	0.9 ± 0.4	0.7 ± 0.3	1.2 ± 0.8	1.7 ± 1.1	-	-
<b>Eosinophils (10<sup>9</sup>/L)</b>	0.1 ± 0.2	0 ± 0	0 ± 0	0 ± 0.1	0 ± 0	-	-
<b>Basophils (10<sup>9</sup>/L)</b>	0.1 ± 0.3	0 ± 0	0.1 ± 0.2	0 ± 0.1	0.1 ± 0.1	-	-

All values expressed as mean ± SD.

$\lambda$  is the coefficient for the power transformation to minimize heteroscedasticity and non-normality

*P* is the result of a one-way ANOVA on transformed data

\*\*\* indicates *P* < 0.001 compared to *WT* with Dunnett's post hoc test

## Figure legends

**Figure 1. cMTFM is due to mutations in G6b-B (G6b).** (A) Family pedigrees. Black arrows point to the probands in each family. Double line indicates a consanguineous relationship. Ages are provided at the time of the initial evaluation of the youngest affected individual in the family. For the deceased proband the age at diagnosis and age of death is listed. (B) Ideograms showing cMTFM linkage region, the *G6b* (*MPIG6B*) locus and patient mutations. (C) Expression of p.Gly157Arg mutant in DT40 cells leads to (C) protein instability and (D, E) reduced expression on the surface of the cell (mean  $\pm$  SEM, n=2). pcDNA3 vector, grey; *G6b-B* WT, green; *G6b-B* p.Gly157Arg, red, MFI, median fluorescence intensity, representative blots and histograms of two independent experiments.

**Figure 2. Pathology of cMTFM.** Wright-Giemsa stained peripheral blood smears from (A) a normal control, (B) patient 3-II-4 and (C) the clinically unaffected, genotypically *G6b*-mutated individual 1-III-9. Note the large, hypogranular platelets (arrow) and RBC anisocytosis in 3-II-4 and the rare giant platelet in 1-III-9 (arrow). Serial histologic sections of a bone marrow biopsies from (D, G, J, M) a normal control individual, (E, H, K, N) 3-II-4, and (F, I, L, O) 1-III-9 stained with (D-F) H&E, (G-I) Reticulin, (J-L) the megakaryocytic marker CD61, and (M-O) G6b-B. Atypical megakaryocytes present in stellate clusters associated with increased reticulin staining are characteristic of cMTFM. Staining for G6b-B is entirely negative in the megakaryocytes and platelets from 3-II-4 and 1-III-9.

**Figure 3. Expression of G6b isoforms in humanized mouse model.** (A) WT, *G6b*<sup>hu/+</sup>, *G6b*<sup>hu/hu</sup>, human and *G6b*<sup>-/-</sup> washed platelet lysates ( $4 \times 10^8$ /mL), were resolved by SDS-PAGE and custom antibodies used to detect mouse (m)G6b-B, human (h)G6b-B and hG6b-A. Expression was quantified and normalized to (i) WT or (ii, iii) human lysates, to show relevant

expression levels in the mouse models. (B) Quantification of glycosylated and unglycosylated human G6b-A and -B, data normalized to show percentage of total expression. (C) hG6b-B was immunoprecipitated (IP) from basal and collagen activated *G6b<sup>hu/hu</sup>* and human washed platelet lysates ( $4 \times 10^8$ /mL). Co-IP of Shp1 and Shp2 was investigated by (i) SDS-PAGE before (ii) quantification and normalization to hG6b-B levels. Quantification was completed using Licor Odyssey system. All data represented as mean  $\pm$  SEM (n=3-4), \*\*\*  $P < 0.001$ .

**Figure 4. Minor alterations of *G6b<sup>hu/hu</sup>* platelet functional responses.** (A) Averaged aggregation and ATP release traces for washed platelets ( $2 \times 10^8$ /mL) activated with indicated concentrations of CRP and anti-CLEC-2 antibody (Ab). Area under the curve (AUC) quantification of (iii) platelet aggregation and (iv) ATP release (n=5-6 per condition, \*\*  $P < 0.005$  and \*  $P < 0.05$ ). (B) Heparin-PPACK-fragmin anti-coagulated whole blood was flowed over glass coverslips coated with collagen immediately following collection. (i) Brightfield images were immediately collected, followed by staining with PE-conjugated JON/A, FITC-conjugated P-selectin and Alexa647-conjugated Annexin V and fluorescence imaging. Analysis quantifying (ii-vi) thrombus surface area coverage and morphological scores of adhered platelets, (n=5-6, \*\*\*  $P < 0.001$ , \*\*  $P < 0.005$ ) and (vii-ix) surface area coverage of fluorescently labeled antibodies (n=5-6, \*\*\*  $P < 0.001$ , \*  $P < 0.05$ ). (C) Total blood loss to body weight ratio of mice following excision of tail tip (n=12-16, \*\*\*  $P < 0.001$ , \*\*  $P < 0.005$ ). All data collection and analysis in panels B and C were completed blinded, mean  $\pm$  SEM, scale bar: 10  $\mu$ m

**Figure 5. Altered tyrosine phosphorylation in response to GPVI and CLEC-2 agonists in *G6b<sup>hu/hu</sup>* platelets.** Representative blots (n=3) of lysates prepared from washed platelets ( $4 \times 10^8$ /mL) activated with indicated concentrations of (A) CRP (90 s, 10  $\mu$ M Iotrafiban, 10  $\mu$ M indomethacin and 2 U/ml apyrase) or (B) CLEC-2 Ab (300 s, 10  $\mu$ M Iotrafiban) and probed with

the indicated antibodies. Src family kinase (SFK) phosphotyrosine (pTyr)418 and Syk pTyr519/20 were quantified using ImageJ and normalized to total tubulin and Syk reblots, respectively.

**Figure 6. Further reduction in hG6b-B expression exacerbates observed phenotype.** (A) *G6b<sup>hu/hu</sup>* mice were crossed with *G6b<sup>-/-</sup>* mice to produce hemizygous (*G6b<sup>hu/-</sup>*) mice. (ii) Representative blots and (iii) quantification of hG6b-B expression in the indicated genotypes (n=3). (B) Average aggregation and ATP release traces and quantification of area under the curve (AUC) investigating functional response of *G6b<sup>hu/-</sup>* mouse washed platelets ( $2 \times 10^8$ /mL) in response to indicated agonists (n=5-6, \*\*\*  $P < 0.001$ , \*  $P < 0.05$ ). All bar graphs presented as mean  $\pm$  SEM.

**Figure 1**

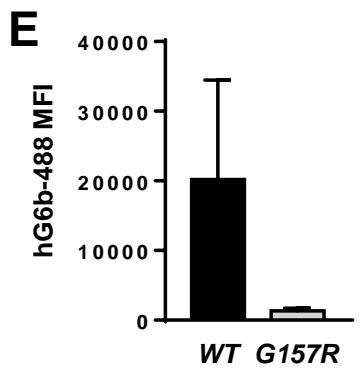
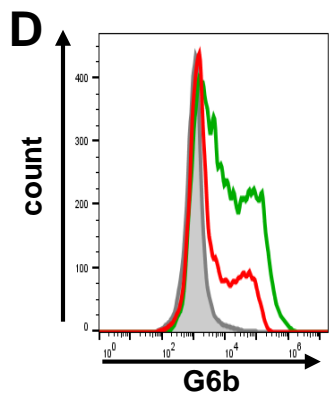
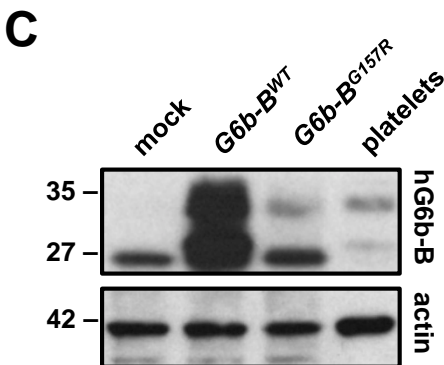
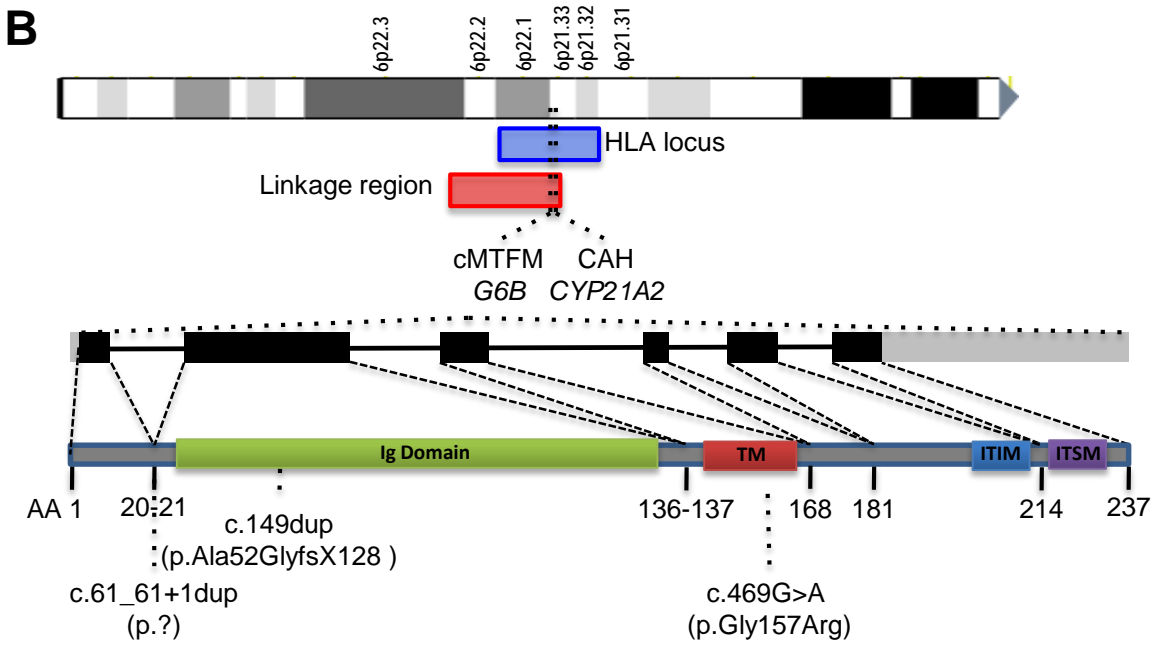
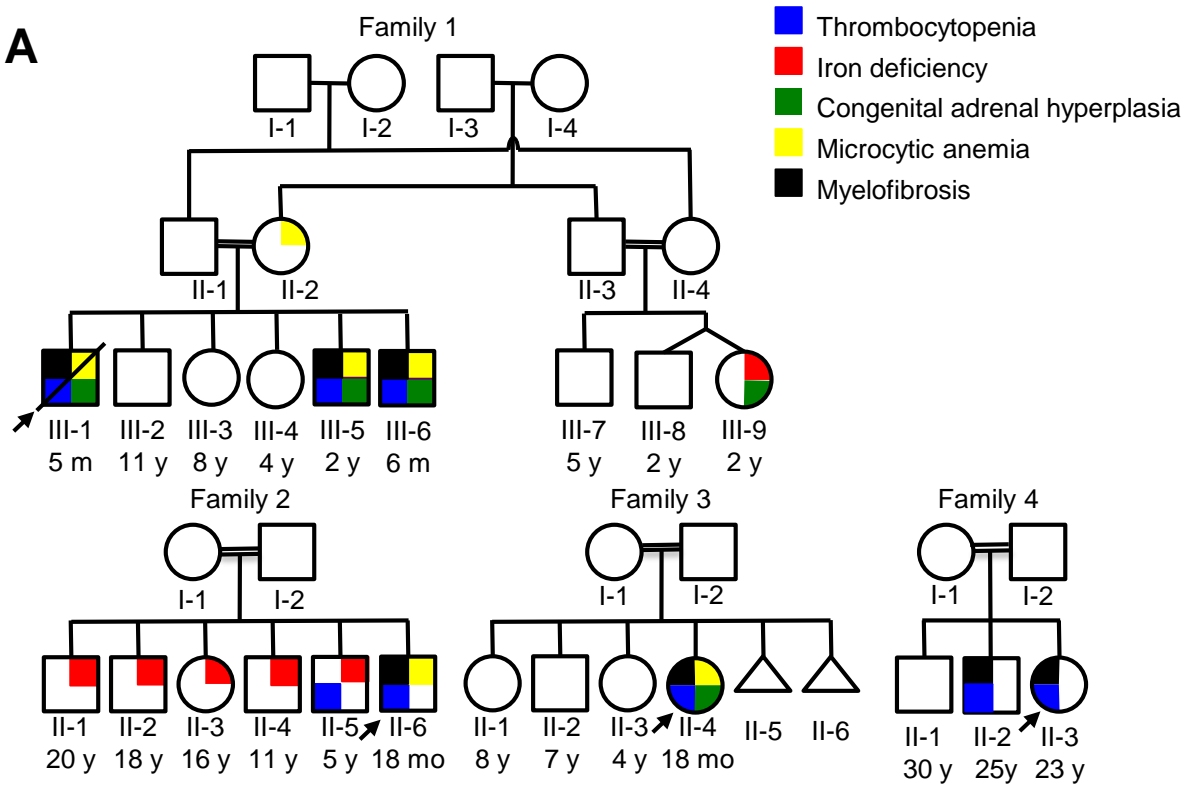


**Figure 2**

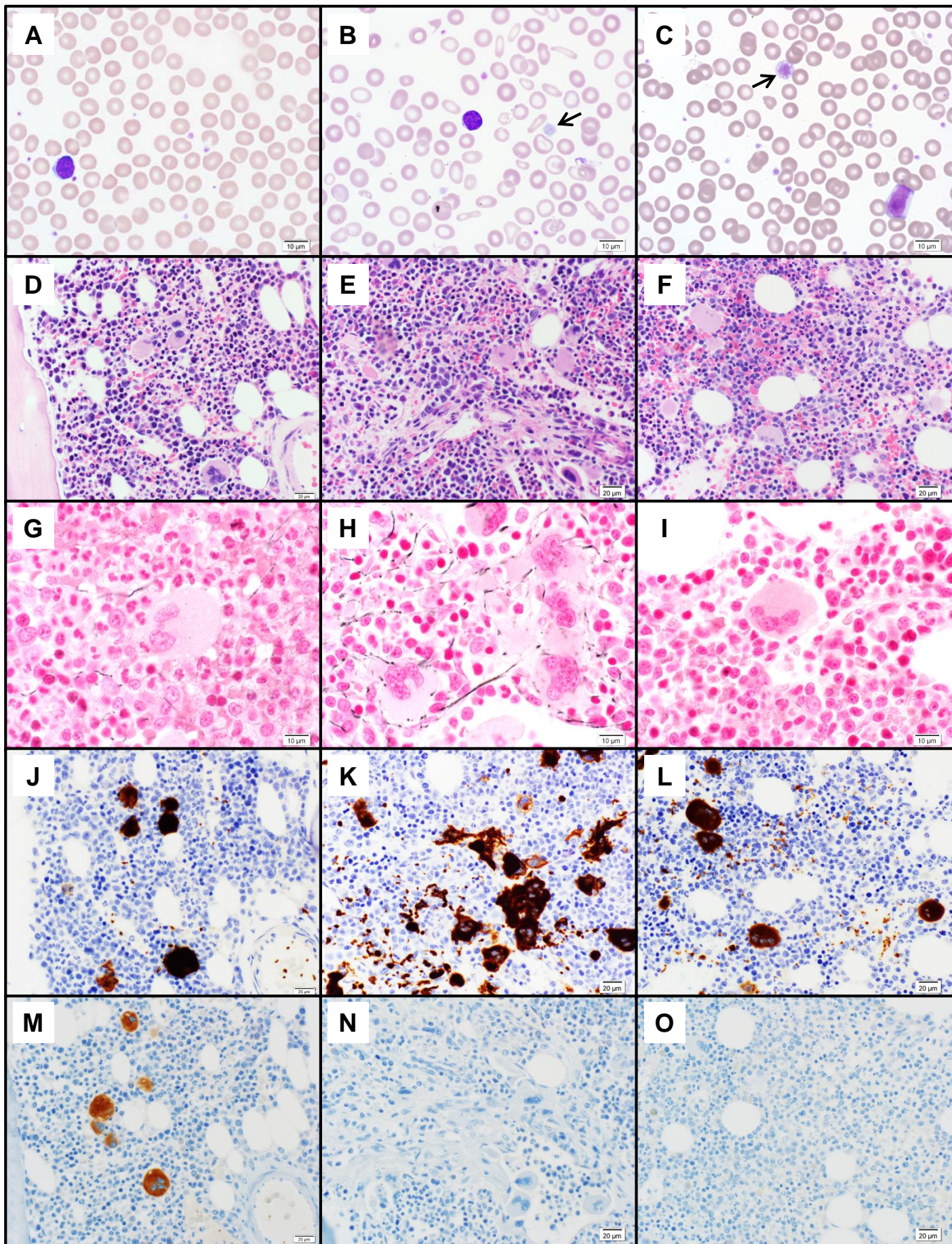


**Figure 3**

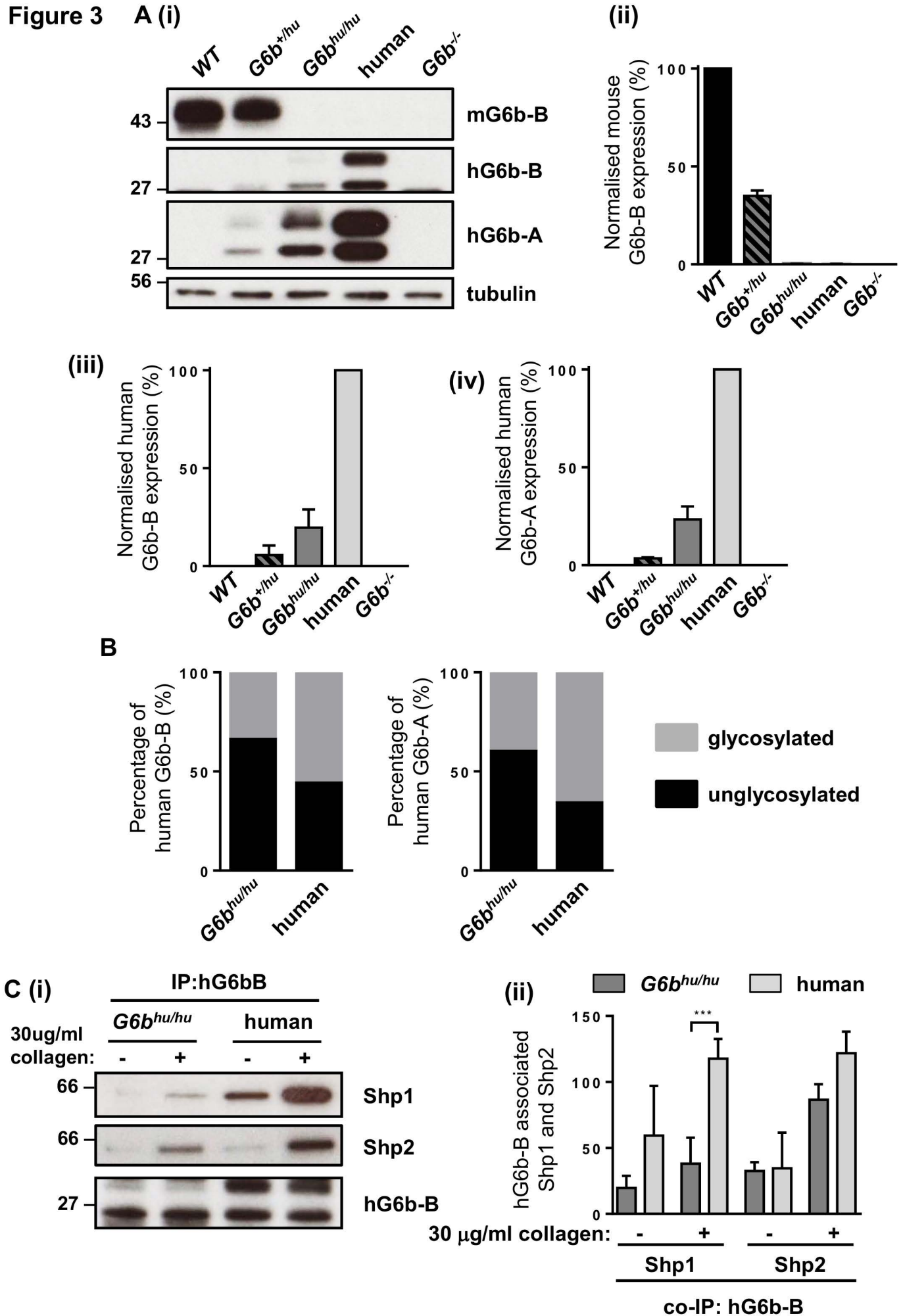


**Figure 4**

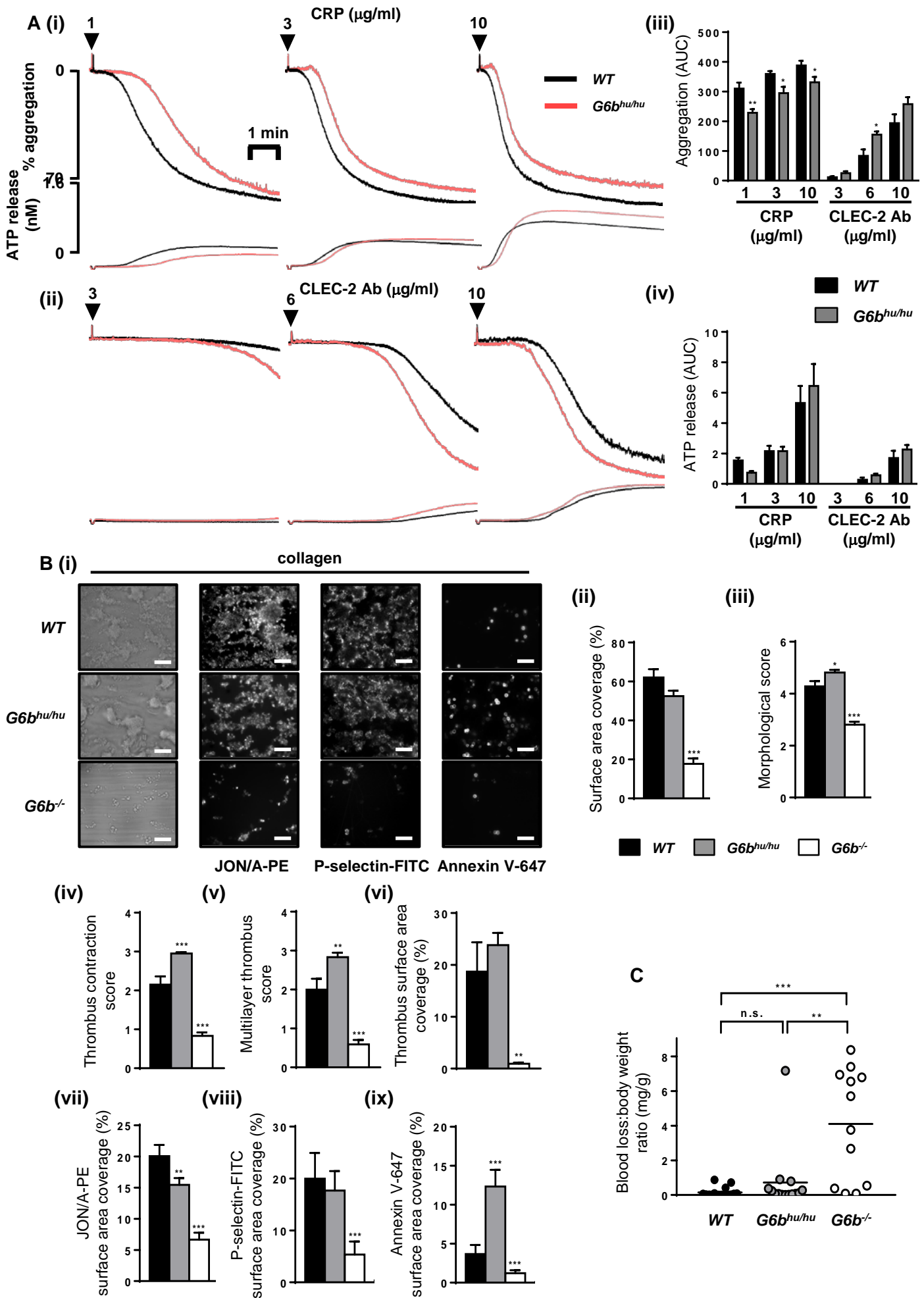
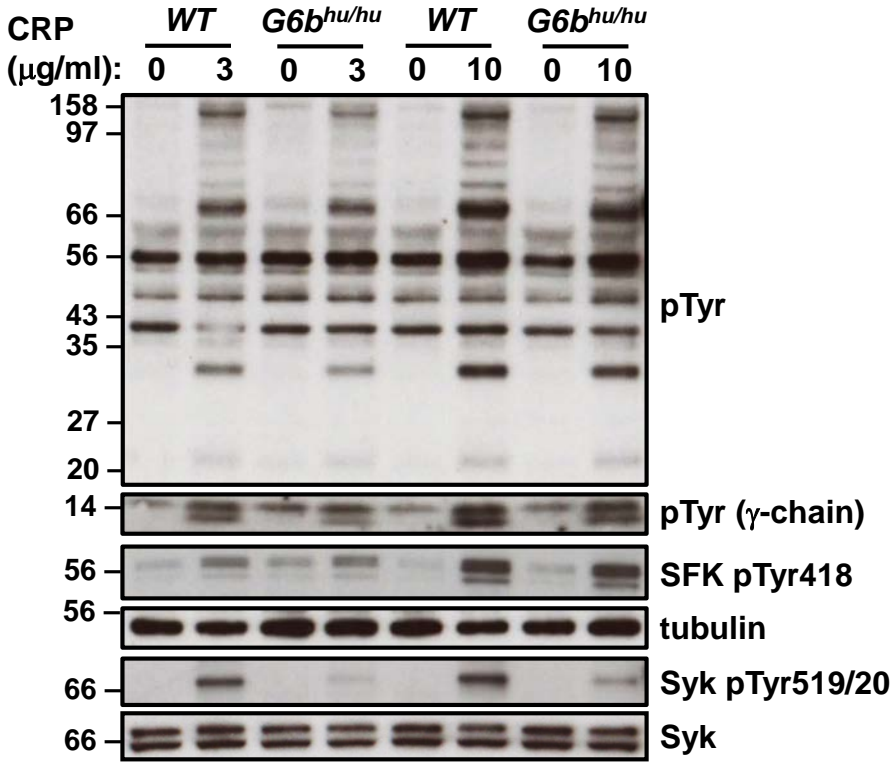
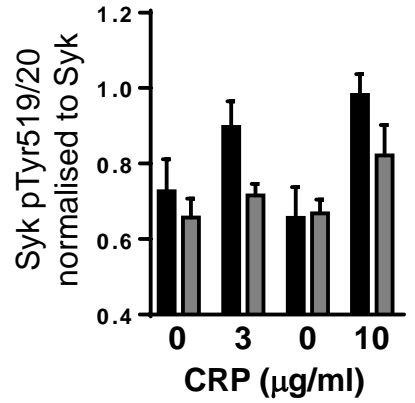
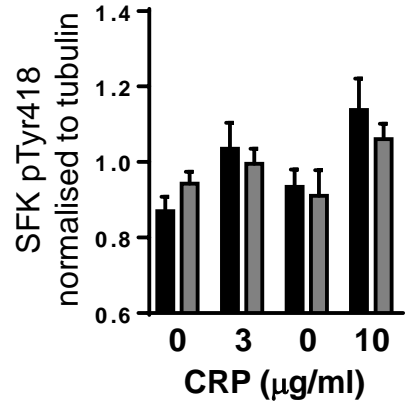


**Figure 5**

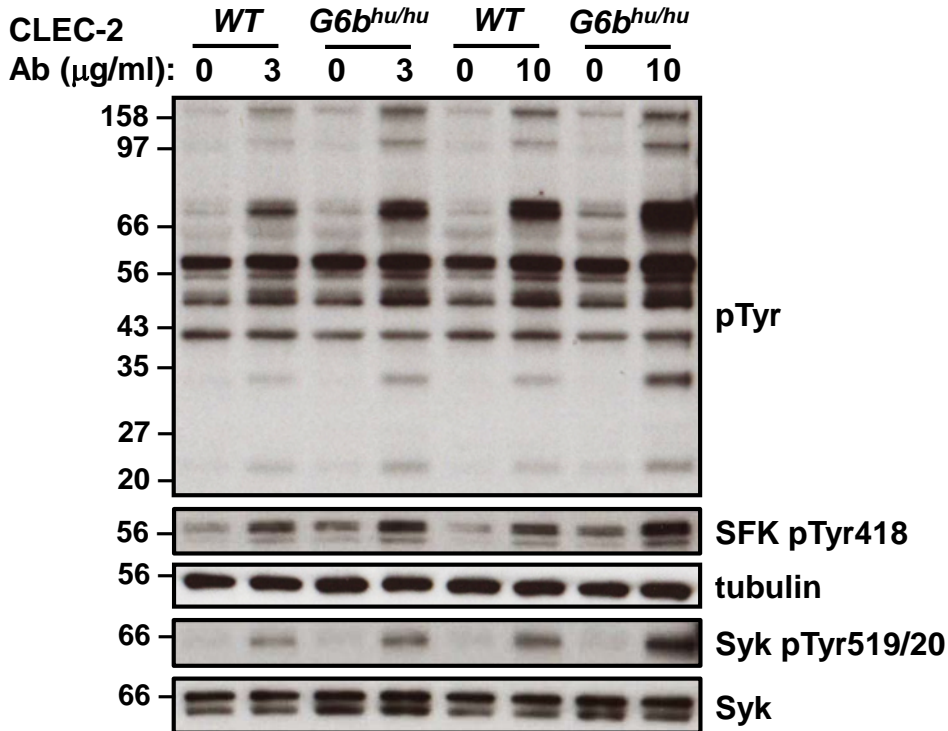
**A (i)**



**(ii)**



**B (i)**



**(ii)**

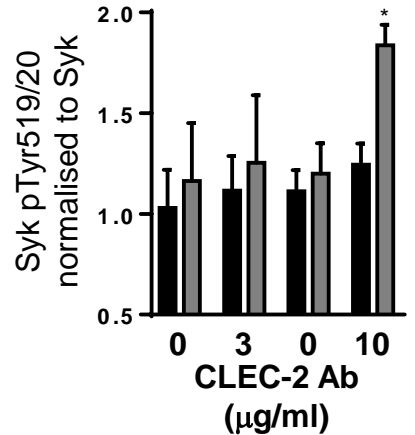
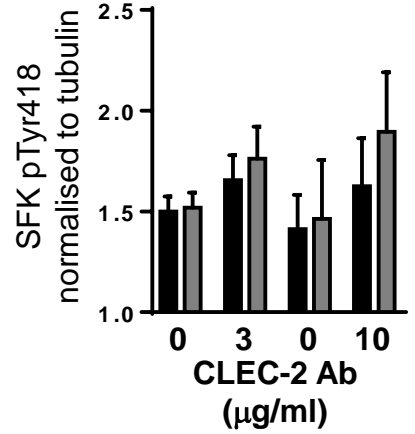
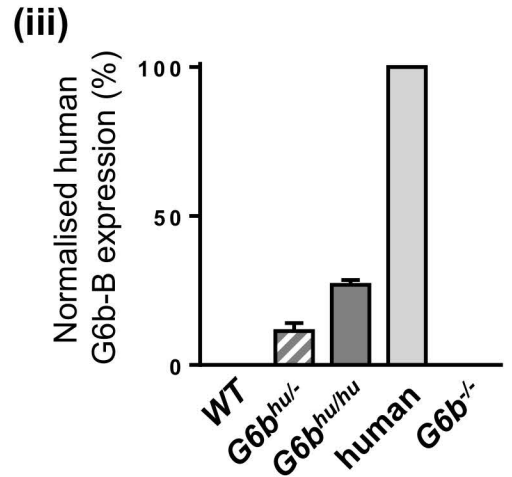
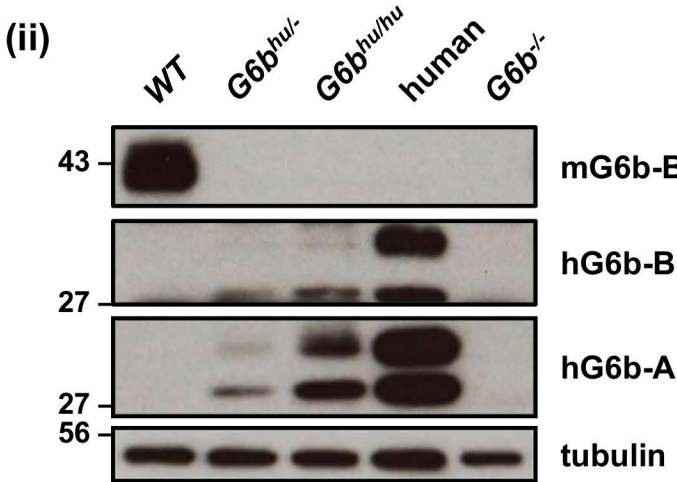
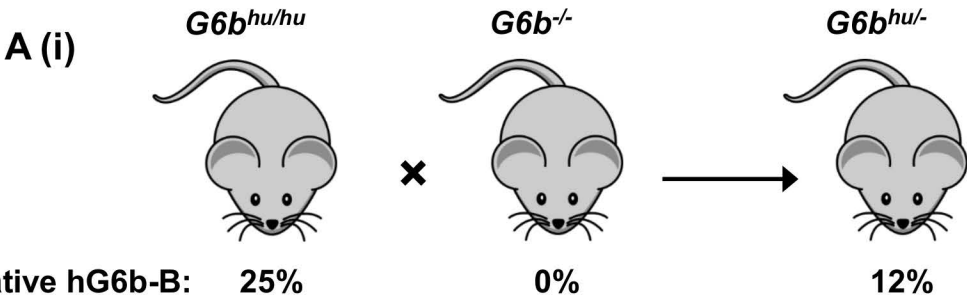
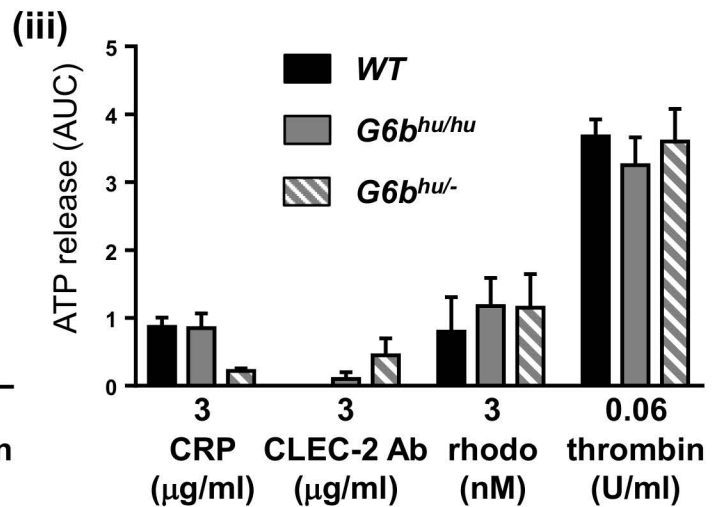
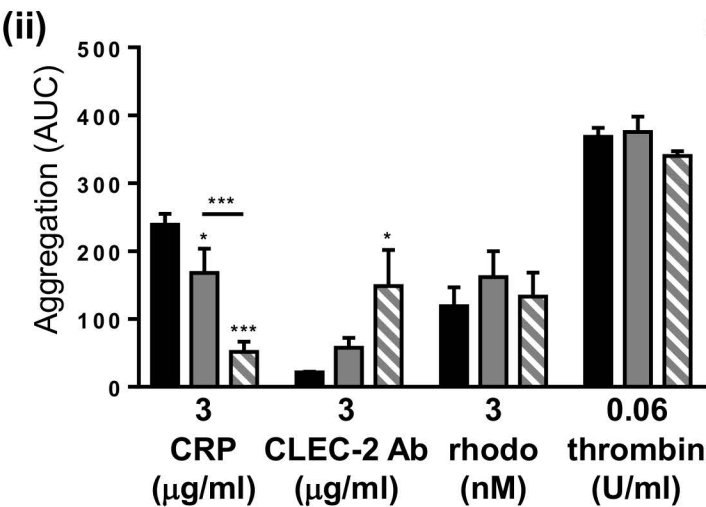
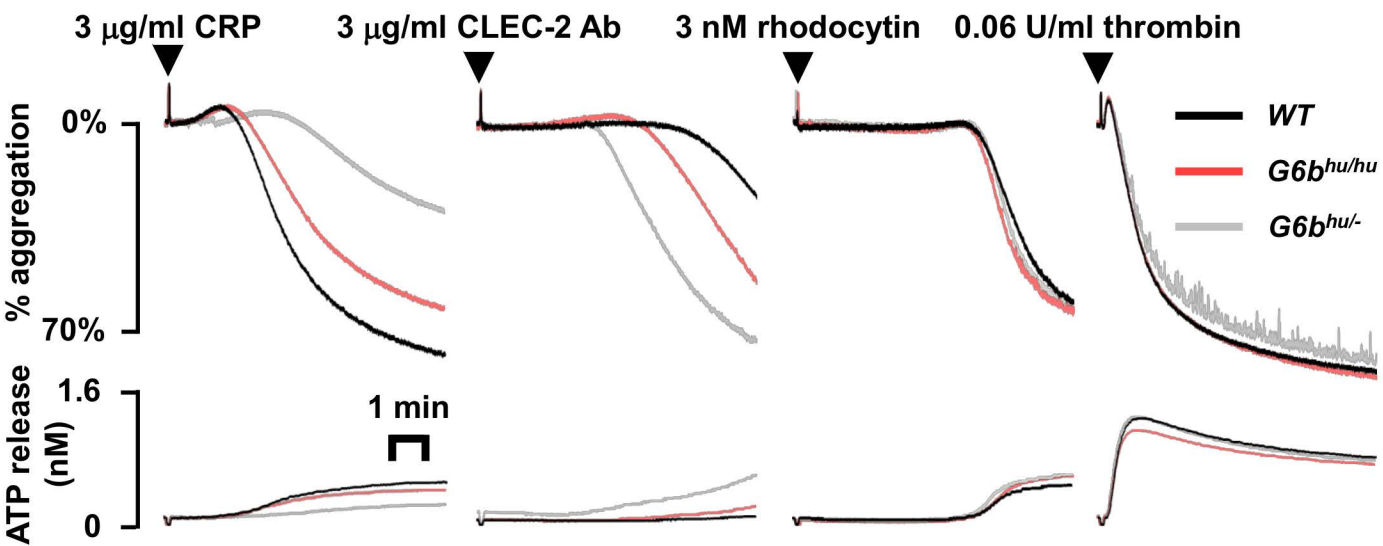


**Figure 6**



**B (i)**





**blood**<sup>®</sup>

Prepublished online June 13, 2018;  
doi:10.1182/blood-2017-08-802769

## **Congenital macrothrombocytopenia with focal myelofibrosis due to mutations in human G6b-B is rescued in humanized mice**

Inga Hofmann, Mitchell J. Geer, Timo Vögtle, Andrew Crispin, Dean R. Campagna, Alastair Barr, Monica L. Calicchio, Silke Heising, Johanna P. van Geffen, Marijke J. E. Kuijpers, Johan W.M. Heemskerk, Johannes A. Eble, Klaus Schmitz-Abe, Esther A. Obeng, Michael Douglas, Kathleen Freson, Corinne Pondarré, Rémi Favier, Gavin E. Jarvis, Kyriacos Markianos, Ernest Turro, Willem H Ouwehand, Alexandra Mazharian, Mark D. Fleming and Yotis A. Senis

---

Information about reproducing this article in parts or in its entirety may be found online at:  
[http://www.bloodjournal.org/site/misc/rights.xhtml#repub\\_requests](http://www.bloodjournal.org/site/misc/rights.xhtml#repub_requests)

Information about ordering reprints may be found online at:  
<http://www.bloodjournal.org/site/misc/rights.xhtml#reprints>

Information about subscriptions and ASH membership may be found online at:  
<http://www.bloodjournal.org/site/subscriptions/index.xhtml>

---

Advance online articles have been peer reviewed and accepted for publication but have not yet appeared in the paper journal (edited, typeset versions may be posted when available prior to final publication). Advance online articles are citable and establish publication priority; they are indexed by PubMed from initial publication. Citations to Advance online articles must include digital object identifier (DOIs) and date of initial publication.